Interactive visualization of curvature flows

Sage Binder
sage-binder@uiowa.edu
Dept. of Computer Science
University of Iowa
Iowa City, Iowa 52242, USA

Matthias Kawski[†]
kawski@asu.edu
School of Math. & Stat. Sciences
Arizona State University
Tempe, AZ 85287, USA

Abstract

After a short motivation, we introduce several different curvature flows: A naive flow on the curvature under the heat equation, the curve-shortening flow, the mean curvature flow for imbedded surfaces, and the Ricci flow on surfaces of revolution and for abstract 2-manifolds. The main focus is on interactive visualizations using animations of curves, surfaces, and in the case of the Ricci also using flow on a metric field similar to Tissot's indicatrix. We refer to and briefly demonstrate an existing applet for the curve-shortening flow, and present our own code written in SageMath / Python (and MAPLE) for other flows, including for the Ricci flow on surfaces of revolution, thus recreating animations first presented by Rubinstein and Sinclair. Our code is publicly available on GitHub and invites for further experimentation, especially with different initial shapes.

1 Introduction

Curvature flows are a beautiful mathematical topic and are under intense study in much cutting edge current research, while they are also very tangible and accessible to even school students in the form of science experiments with soap bubbles and films [14]. Calculus students are familiar with problems of minimizing area given a perimeter constraint. The classical version that does not limit itself to rectangles is the isoperimetric problem or Dido's problem which has had a huge impact on mathematics, and is a first example in the study of calculus of variations. [3]. Rather than just looking at static minimal (networks of) curves and surfaces, it is natural to try to continuously deform arbitrary such into minimal ones. Great models for the way nature does this are various notions of *curvature flows*. The main idea is that curvature should spread out, just like a giant soap bubble evolves towards having everywhere constant curvature, eventually becoming a sphere. Similarly to temperature evolving on a metal plate, with hot spots becoming cooler, and cold spots warming up. Eventually, the temperature variations on the plate should *diffuse* and eventually yield a constant temperature. Indeed, many curvature flows are solutions of partial differential equations that somewhat look like the heat, or diffusion

[†]Corresponding author

equation $u_t = u_{xx} + u_{yy}$ – but with the second partials replaced by nonlinear functionals of $u = u(t, x, y)$ that involve various notions of curvature of the graph or surface.

Curvature flows have been highly publicized in the past 25 years, especially Hamilton's Ricci flow that Perelman utilized to prove the Poincaré conjecture [21]. However, the Ricci flow is a highly abstract flow lives on abstract manifolds, and is is very inaccessible to non-experts. Our objective is to present several notions of curvature flows that share fundamental underlying properties, yet are much more accessible and tangible than the general Ricci flow.

In general, differential geometry distinguishes between extrinsic and intrinsic properties of curves, surfaces, and manifolds. Roughly speaking, the curvature of a space curve and the mean curvature of a smooth surface in 3-space are extrinsic because they depend on how the curve or surface is imbedded in the ambient (surrounding) 3-space. On the other hand, the Gauss and Ricci curvature only depend on the metric, that is, the infinitesimal notion of distance. For example, the Gauss curvature, and geodesics (shortest curves) on a sheet of paper do not change no matter whether the paper is rolled into a cylinder, or cone, or lies flat on a table. The next more intriguing examples are flat tori and Klein bottles that are *constructed* (in our minds) by identifying (gluing together) opposite sides of a square in the plane (without or with reversing orientation). Nonetheless, given the original notion of distance in the plane (accommodating crossing the glued together edges like in a Pac-Man game), one still has well-defined notions of geodesics, namely straight lines in the rectangle picture. With their zero Gauss curvature, these abstract surfaces that cannot be imbedded in 3-space while preserving the original metric, or notion of distance.

We start with simple experiments with plane curves evolving under different kinds of curvature flows. Then we give some brief remarks about the *extrinsic* well-known curve-shortening and mean-curvature flow for curves and surfaces, respectively. Continuing our main focus is on *intrinsic* geometric flows, we experiment with the Ricci flow for two-dimensional surfaces in the very special case of surfaces of revolution. Throughout, the focus is presenting tools, and discussing their use for interactive visualization of the ensuing deformations. Data are generally assumed to be smooth, i.e., having continuous (partial) derivatives of all orders, unless specified otherwise.

2 A simple model at the level of multi-variable calculus

According to the fundamental theorem of curves every smooth immersed (i.e., everywhere nonzero derivative) curve $\gamma\colon I \mapsto \mathbb{R}^2$ in the plane is, up to Euclidean motions (translations and rotations) completely determined by its curvature.

We illustrate how to recover the curve from its curvature, and then animate many examples, especially closed curves that straighten out to become circles. [In the literature, length constrained curvature flows are discussed primarily as a modification of the curve-shortening flow (see the next sections), e.g., [18].]

Throughout I stands for an interval, ray or $\mathbb{R}$ or the circle $I = S^1$. Without loss of generality, we assume that γ is parameterized by arclength, customarily denoted by s, and thus $|\gamma'| = 1$. Denoting the (unit) tangent vector $T = \gamma'\colon I \mapsto \mathbb{R}^2$, for plane curves it is customary to define a unit normal vector field $N\colon I \mapsto \mathbb{R}^2$ along γ such that $\{T, N\}$ is positively oriented, i.e., with common abuse of notation $\det(T|N) = +1$. With this, the *signed* curvature of plane curves is defined as $\kappa\colon I \mapsto \mathbb{R}$ by $\kappa = \langle \gamma'', N\rangle$ where $\langle \cdot, \cdot rangle$ is the standard inner product on $\mathbb{R}^2$.

Given any smooth function $\kappa\colon I \mapsto \mathbb{R}$ and initial data $\gamma(0) = p \in \mathbb{R}^2$ and $\gamma'(0) = (\cos\theta_0, \sin\theta_0)$ for some $\theta_0 \in \mathbb{R}$, the first antiderivative yields for $s \in I$ and $|s|$ sufficiently small $\theta(s) = \int_0^s \kappa(\sigma)\, d\sigma$. Note, that $\kappa\colon S^1 \mapsto \mathbb{R}$ *periodic* does not imply that its antiderivative θ is periodic. A further integration yields a parameterized curve $\gamma\colon I \mapsto \mathbb{R}^2$ (with the same caveat about periodicity as above) that is the unique curve (parameterized by arclength) whose curvature function agrees with κ.

A few suggestions for interactive classrooms:

- Start with the traditional *straightforward* direction: Given a formula for a curve, plot it and propose what the graph of κ may look like. Then use basic differential calculus (using the usual formulas for curves not necessarily parameterized by arclength) to calculate its curvature, and plot it to confirm the guess – or elaborate what mistakes were made.
- Given a sketch of the graph of κ try to sketch a curve whose curvature looks like κ. Confirm using computing technology such as our Sage-applet or MAPLE-worksheet. Typical examples for the curvature $\kappa(s)$ should/may include (for constants a, b, $c \in \mathbb{R}$ with various signs) $\kappa = c$, $\kappa\colon s \to c + a\cos bs$, $\kappa\colon s \to a/(b+s)$ for $s > -b$, and $\kappa\colon s \to a/(1+bs^2)$. In the latter, pay special attention to the graphical meaning of $\int_{-\infty}^{\infty} \kappa(\sigma)\, d\sigma$.

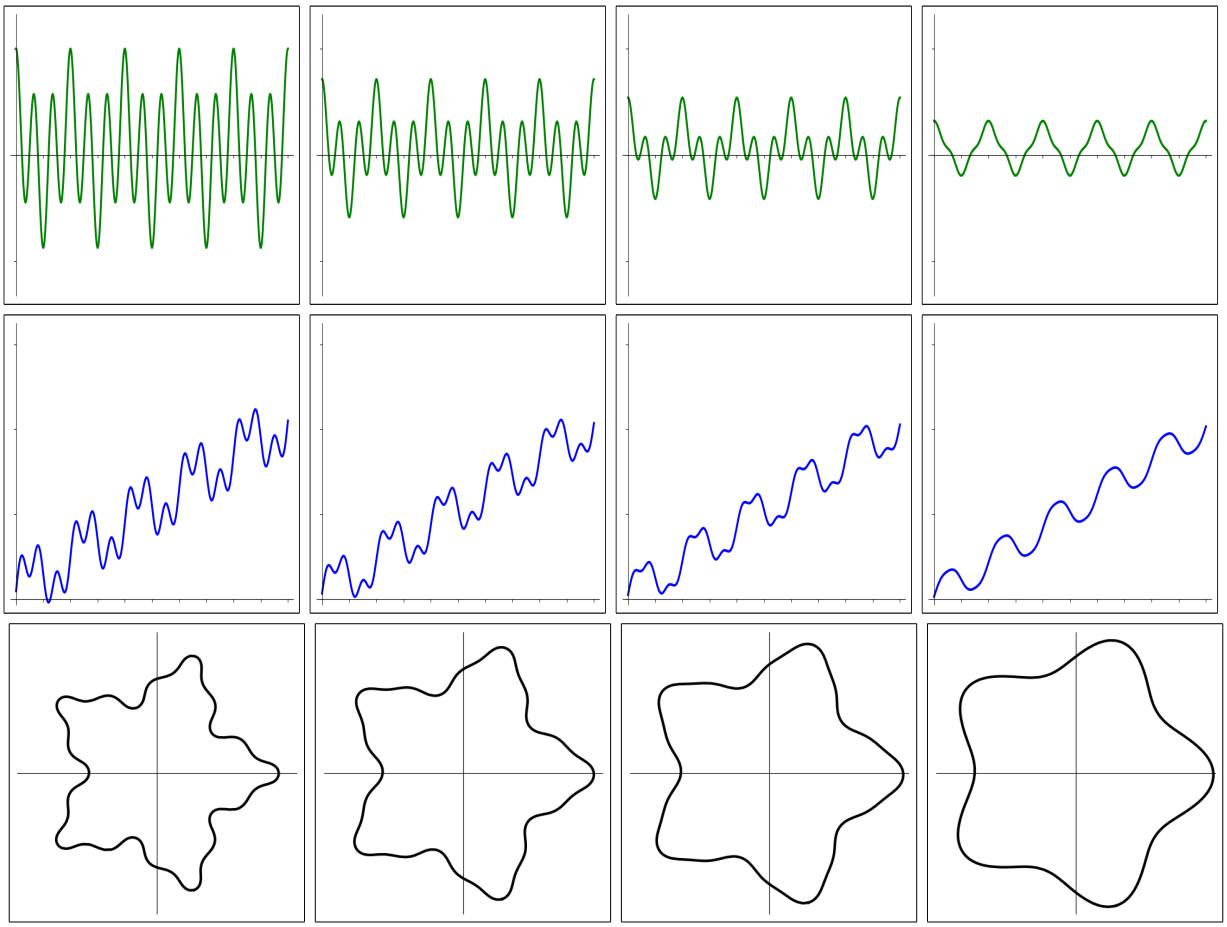

Figure 1: Curvature flow on closed curves with fixed length. Time increases left to right.

Calculations involving arc-length are notoriously hard to complete within the traditional set of elementary functions. This is a good place to explore what computer algebra can do, and else explore the trustworthiness of naive numerical approximations using popular computing packages or applets like the one we provide.

After this *warm-up* let us get started with curvature flows. Instead of considering individual curves, in general much more insight is gained by considering parameterized families of curves. The above with a, b, $c \in \mathbb{R}$ are typical algebraic examples. Here and in the sequel we want to consider a single parameter $t \in J \subseteq \mathbb{R}$ which we identify with the tangible notion of time. Technically for some $T \in (0, \infty]$ consider smooth functions $\gamma\colon [0, T) \times I \mapsto \mathbb{R}^2$ and the corresponding $\kappa\colon [0, T) \times I \mapsto \mathbb{R}$.

Similar to the much better known and well-studied case of the curve-shortening flow (which we briefly address in the next section), one simple idea is to ask that curvature *spreads out*, *tries to equalize*: Short, highly curved segments try to straighten out by pushing some of their curvature to neighboring segments. For curves with a *fixed total length* (i.e. fixed domain I) this suggests posing the diffusion (or heat) equation: The rate of change of curvature with time is a positive multiple of the second derivative of curvature with respect to its natural parameter arclength $s \in I$ (using subscripts to denote partial derivatives)

$$\kappa_t = c\, \kappa_{ss} \tag{1}$$

This very simple example is accessible to multivariable calculus students. Indeed, in the second author's multivariable classes, students routinely use EXCEL worksheets to estimate numerical derivatives and explain their meaning – and usually culminating in numerically solving the heat equation and graphically observing *diffusion* of hot and cold spots.]

Unlike the much more involved curve-shortening flow addressed in the next section, this is just the elementary *linear* heat equation.

The first examples suggested in the above *warm-up* provide good starting conditions – make sure that before doing any computations to test your (and your students) intuition and sketch the graphs of the evolving curvature functions and their corresponding curves.

We find that some of the most attractive introductory examples are given by initial curves that are (low order) trigonometric polynomials (or finite Fourier series) such as

$$\kappa(0, s) = a_0 + a_1 \cos s + a_3 \cos 3s. \tag{2}$$

It is a simple exercise to find conditions on the parameters such that the corresponding curve is closed and simple, and indeed attractively look like a flower with many petals. A special advantage of such curves or curvature functions is that the solution of the diffusion equation (1) can easily be written out in closed form using the routine separation of variables technique (for suitable boundary data)

$$\kappa(t, s) = a_0 + a_1 e^{-ct} \cos s + a_3 e^{-9ct} \cos 3s. \tag{3}$$

The corresponding computations are very easy to implement using computer algebra, or *sympy*, or numerical integration (e.g., using *numpy*). Typical results are illustrated in figure 1.

Extension: For fun, replace the diffusion equation (1) by the (linear) wave equation to obtain some truly inspiring animations. Note that in this case, the solution can be written down in closed form just as easily as for the diffusion equation. It is immediate to create similar animation with the curvature evolving according to the wave equation, reminiscing the motions undergone by giant soap bubbles mentioned in the discussion.

3 Curve Shortening Flow

A common basic question is: "How do physical curves and surfaces and surfaces evolve with time if for example the driving force is given by *surface tension*?" In the case of soap bubbles, modeling surface tension as proportional to surface area, with an the apparent objective is minimizing surface area, (or total length) given a fixed volume (or area). The latter objective is well known as Dido's problem (see also: *isoperimetric inequality*).

Intuitively, every point on the image of the curve $\gamma(t\,\cdot\,)$ shall move in the direction normal to the curve (in the convex direction) at a rate proportional to the (signed) curvature at this point, often written as $\frac{\partial}{\partial t}\gamma(t,s) + \kappa(t,s)\,\mathbf{N}(t,s)$. Using standard subscript notation for derivatives, the flow is again generated by the deceptively innocent looking differential equation

$$\gamma_t = c\,\gamma_{ss}. \tag{4}$$

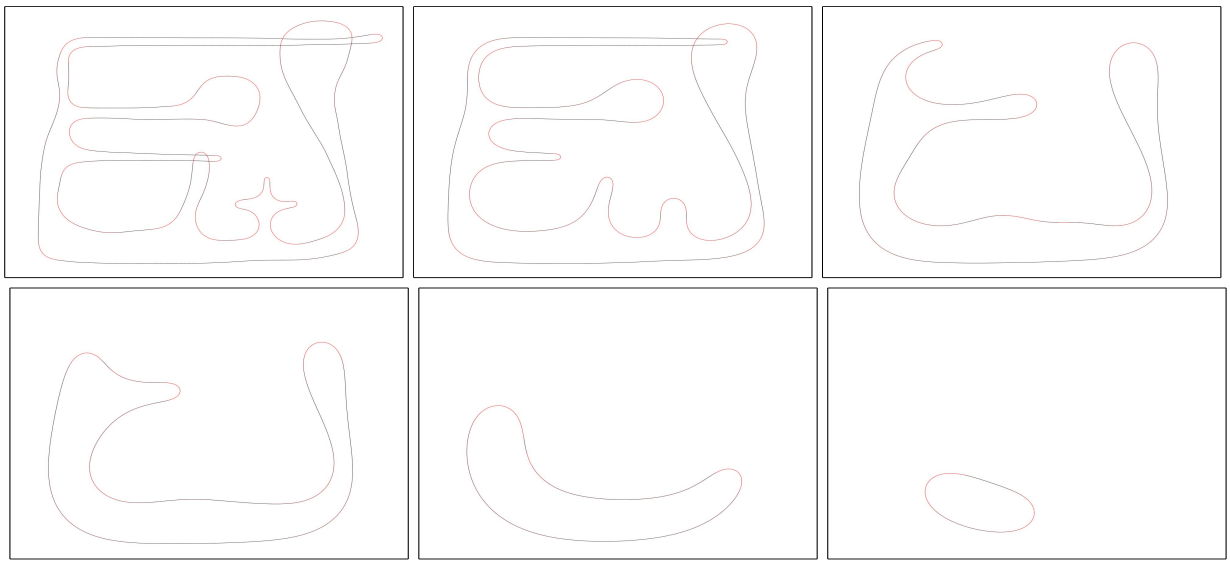

Figure 2: Curve shortening flow: Carapetis' applet

The key observation is that the arclength s of the curve $\gamma(t\,\cdot\,)\colon [0, L(t)] \mapsto \mathbb{R}^2$ depends on the time $t \geq 0$, and thus the partial differential operators $\frac{\partial}{\partial t}$ and $\frac{\partial}{\partial s}$ no longer commute.

We recommend the recent monograph [1] for both a detailed introduction and also a meticulous technical development of properties of the *extrinsic* geometric flows addressed in this and the next section. Most notable is that this flow is the (negative) gradient flow on a space of smooth curves for the length functional (lemma 2.4. in [1]). A central result for the curve shortening flow is the Gage–Hamilton–Grayson theorem, which roughly says that every smooth simple closed curve will remain without self-intersections, become convex, and eventually converge to a *round point*.

While we have no new visualization tools for this flow to present, we highly recommend the wonderful free applet (similar to JavaScript) [8] by A. Carapetis. The user may draw any curve in the plane, and then study the evolution of the curve under the curve shortening flow. Figure 2 provides a simple sequence of screenshots for a simple curve that initially has multiple self-intersections.

4 Mean curvature flow for surfaces

The mean curvature flow on smooth surfaces $\subseteq \mathbb{R}^3$ imbedded in Euclidean space is an *extrinsic* flow that is an intuitive analog of the curve shortening flow discussed in the previous section. From a calculus of variations perspective, it is the (negative) gradient flow on a space of smooth closed surfaces for the volume functional.

Heuristically, every point of the surface moves in the direction of the normal vector (with consistently chosen orientation) at the rate of the mean curvature, usually denoted by H. It is easiest defined via the *extrinsic* Gauss map $\mathbf{N}\colon S \mapsto S^2 \subseteq \mathbb{R}^3$ that assigns to every point p on the surface S a unit normal vector $\mathbf{N}(p)$ (with consistent orientation). The mean curvature is one half the trace of the differential $d\mathbf{N}$, i.e., the average of its eigenvalues κ_i

$$H = \frac{1}{2} \operatorname{tr} d\mathbf{N} = \frac{1}{2}(\kappa_1 + \kappa_2) \tag{5}$$

These are known as the principal curvatures, and they are the minimal and maximal *sectional* curvatures of the curve intersections of the surface with planes that contain the normal line at the given point.

The normalized mean curvature flow that preserves volume is familiar as the *surface tension flow* that models, e.g., the motion of soap bubbles, or more general surfaces of drops of liquids.

The literature on the mean curvature is vast, and we again refer to the monograph [1] for both a detailed introduction and also a meticulous technical development of its properties. Most notable are its close connection with the Laplacian, harmonic analysis, and minimal surfaces defined by the vanishing of $H = 0$.

While smooth closed (uniformly) convex surfaces also shrink into a point, they do so in finite time. However, flows initialized by nonconvex surfaces may develop singularities with the curvature becoming unbounded in finite time, see, e.g., [9]. One of the best known examples is a surface in the shape of a smooth dumbbell whose neck's diameter will shrink much faster than the *radii* of the *sphere like* ends, then *pinch off* in finite time and become two disconnected surfaces. Pictorially, such behavior is reminiscent of the Ricci flow in higher dimensions, and is the opposite of the Ricci flow in two dimensions as illustrated in figure 6. Collapsing solutions of ancient flows (i.e., that exist backwards in time to negative infinity) are investigated in [6], while positive results on the flow through singularities are presented in [2].

5 Riemannian manifolds and the Tissot indicatrix

This section provides a gentle first step beyond multi-variable calculus towards Riemannian manifolds, that will be utilized in the last two sections in the context of the Ricci flow. Multivariable calculus and first differential geometry courses usually only consider smooth two-dimensional surfaces that are imbedded in three-dimensional Euclidean space.

For simplicity, consider the graphs of the functions $f_\pm\colon (x, y) \mapsto x^2 \pm y^2$, illustrated in the images in the top row of figure 3. This computer illustration uses a very coarse 6×6 grid of points (x_i, y_j) in the domain and connects the points $(x_i, y_j, f_\pm(x_i, y_j))$ by line segments whose projections onto the xy-plane from a regular square grid. Contrary to what the filled-in patches in the computer illustration suggest, in general, the four corners of each patch do *not* lie in any plane. But as the number of grid points increases, the patches are better and

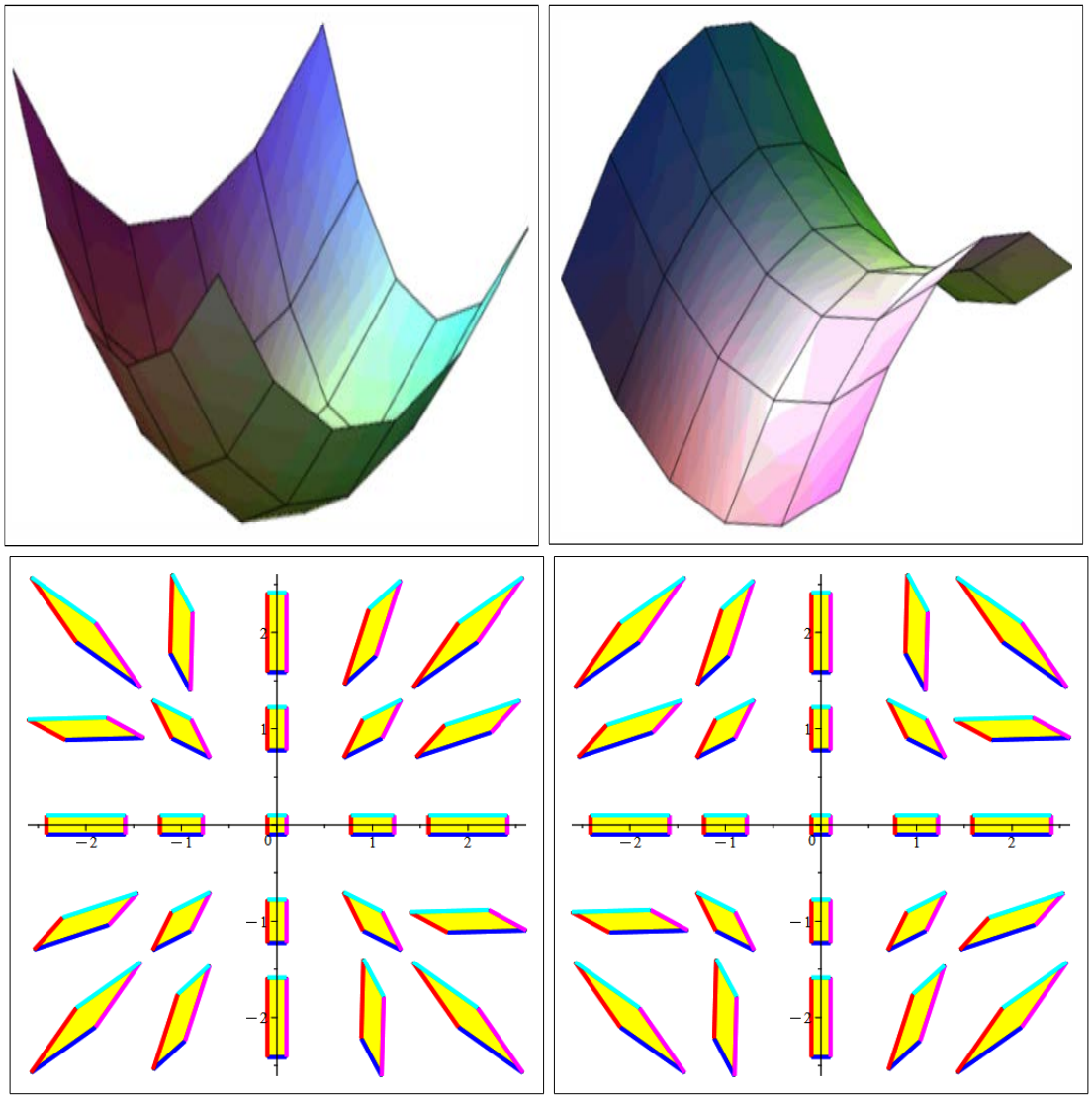

Figure 3: Chopping up surfaces into almost parallelograms

better approximated by (planar!) parallelograms – provided this is the graph of a continuously differentiable function.

Next think of cutting up the surface along these grid lines, and drop the near parallelograms into the plane, as suggested in the images in the bottom row of figure 3. Note that each patch is necessarily at least as large as the $(\Delta x, \Delta y)$ rectangle beneath it, and thus we uniformly rescaled the patches, and chose the orientation to most closely reflect the orientation of the path above in 3-space. This picture shows parallelograms whose sides have lengths identical to the lengths of the averaged opposite sides of the original patch

$$\frac{(x_{i+1}, y_j, f_\pm(x_{i+1}, y_j)) - (x_i, y_j, f_\pm(x_i, y_j)) + (x_{i+1}, y_{j+1}, f_\pm(x_{i+1}, y_{j+1})) - (x_i, y_{j+1}, f_\pm(x_i, y_{j+1}))}{2},$$

$$\frac{(x_i, y_{j+1}, f_\pm(x_{i+1}, y_j)) - (x_i, y_j, f_\pm(x_i, y_j)) + (x_{i+1}, y_{j+1}, f_\pm(x_{i+1}, y_{j+1})) - (x_{i+1}, y_j, f_\pm(x_{i+1}, y_j))}{2}.$$

The key mental exercise is to try to glue (tape) together the respective edges, blue to cyan,

and red to magenta, to recover the original surface in 3-space.

Flattening out the patches into plane parallelograms made the curvature inside each surface patch disappear, or, in fancy terms, *move and concentrate* it along the edges and at the vertices. However, on the larger scale the curvature is still highly visible: Think of the geodesic circles of radius $r > 0$ about the center $(0, 0, 0)$ in either graph, that is, the locus of all points that have the same distance r from the origin. In the case of the elliptic/circular paraboloid $z = x^2 + y^2$ this again a circle. Indeed, for geodesic radius $r = 1$, by calculating the arclength along the arc (t, t^2) we find that the geodesic circle with radius $r = 1$ inside the surface is a circle of radius $\rho \approx 0.7639$ in the plane $z \approx 0.5835$, with circumference less than 2π. Conversely, in the case of the hyperbolic paraboloid $z = x^2 - y^2$ one obtains an undulating curve that indeed has a circumference exceeding $2\pi r$. Indeed, these reflect that the elliptic and hyperbolic paraboloids have strictly positive and strictly negative Gauss curvature, respectively.

What matters for us is that by visually patching/gluing together families of parallelograms, it appears quite clearly that in the first case the resulting surface curves to form a bowl shape (possibly upside down), while in the case there is extra length to be used up, which results in an undulating surface such as a saddle.

We continue with a few introductory remarks about abstract manifolds and Riemannian metrics. As the first step, smooth manifolds may be thought of as generalizations of smoothly parameterized curves and surfaces in the plane or in 3-space, but now parameterized by n parameters and being *surface-like* objects in some high dimensional space $\mathbb{R}^N$. Indeed, due to Whitney's and Nash's imbedding theorems (compare the next section), this is a totally legitimate view. However, the modern view considers abstract (differentiable) manifolds as general (topological) spaces. The principal requirements are that every point is contained in a *local coordinate chart* which is an open neighborhood together with a local diffeomorphism onto (an open subset) of a Euclidean space, together with some compatibility condition of overlapping charts. The local diffeomorphism is called a system of local coordinates, and may be thought of as the inverse of a *local parameterization*, as in multivariable calculus.

Whereas traditional surfaces inherit a notion of distance from the ambient (surrounding) space, one endows abstract manifolds with abstract Riemannian metrics (typically, in physical settings, interpreted as energy or momentum *tensors*) which in turn provide inner products on the tangent spaces of the manifold. For a two-dimensional manifold, such a Riemannian metric may be considered (in local coordinates) as a smooth positive definite two-by-two matrix valued functions on the manifold.

As simple examples for Riemannian metrics (using notation similar to [11]) consider a sphere and a hyperbolic paraboloid imbedded in $\mathbb{R}^3$ with (local and global) parameterizations defined by $\mathbf{x}\colon (-\pi, \pi) \times (0, \pi) \mapsto \mathbb{R}^3$ and $\mathbf{y}\colon \mathbb{R}^2 \mapsto \mathbb{R}^3$,

$$\mathbf{x}(\theta, \phi) = (\cos\theta \sin\phi, \sin\theta \sin\phi, \cos\phi), \quad \text{and} \quad \mathbf{y}(u, v) = (u, v, u^2 - v^2). \tag{6}$$

In these cases the induced Riemannian metrics (or first fundamental forms) are represented by 2×2 matrices, in various notations

$$\begin{pmatrix} E & F \\ F & G \end{pmatrix} = \begin{pmatrix} g_{11} & g_{12} \\ g_{21} & g_{22} \end{pmatrix} = J^T J, \tag{7}$$

where J is either of the Jacobian matrices of partial derivatives

$$J_1 = \left(\frac{\partial \mathbf{x}(\theta,\phi)}{\partial(\theta,\phi)}\right) = \begin{pmatrix} -\sin\theta\sin\phi & \cos\theta\cos\phi \\ \cos\theta\sin\phi & \sin\theta\cos\phi \\ 0 & -\sin\phi \end{pmatrix} \quad \text{and} \quad J_2 = \left(\frac{\partial \mathbf{y}(u,v)}{\partial \mathbf{y}(u,v)}\right). = \begin{pmatrix} 1 & 0 \\ 0 & 1 \\ 2u & -2v \end{pmatrix} \tag{8}$$

$$g_{\mathbf{x}} = J_1^T J_1 = \begin{pmatrix} \sin^2\phi & 0 \\ 0 & 1 \end{pmatrix} \quad \text{and} \quad g_{\mathbf{y}} = J_2^T J_2 = \begin{pmatrix} 1+4u^2 & -4uv \\ -4uv & 1+4v^2 \end{pmatrix} \tag{9}$$

The columns of the Jacobians J visually correspond to velocity or tangent vectors along the grid lines (coordinate curves) of the parameterized surface. Their inner products in $J^T J$ and entries g_{ij} of the Riemannian metric correspond to their lengths (squared) and the angle between the velocity vectors.

We would like to visualize the metric *field* g (a matrix valued functions of the parameters (u, v)). Instead of drawing two arrows at each point (u, v) corresponding to the column vectors of $g(u, v)$, our eye find it easier to consider the parallelogram at each point (u, v) spanned by these column vectors.

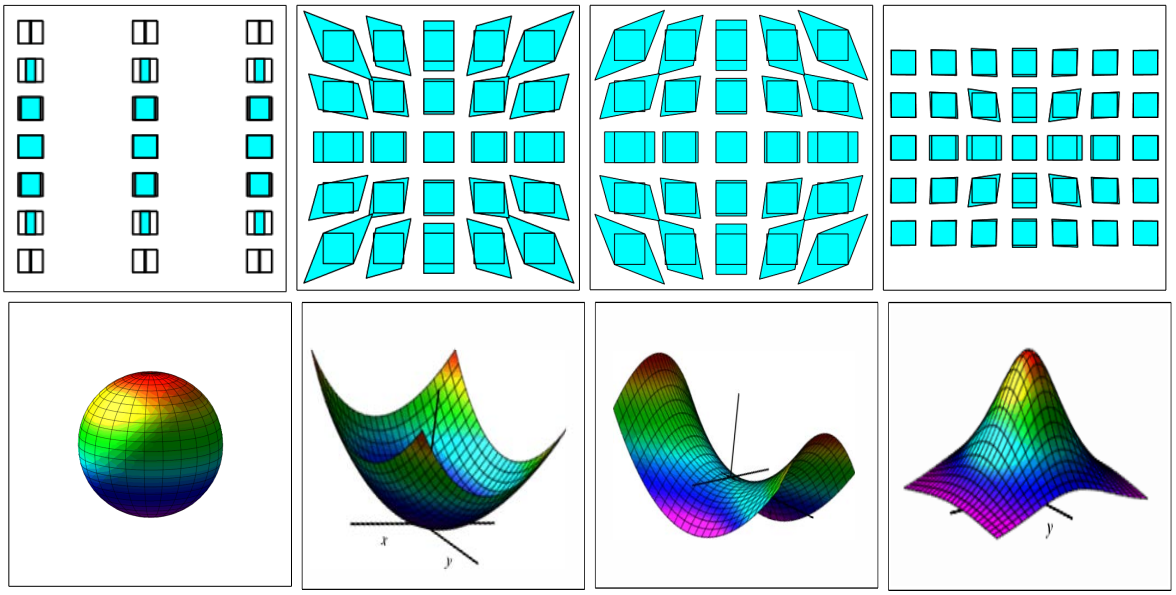

Figure 4: Squint your eyes: Riemannian metrics and surfaces

Indeed, when replacing g in the above discussion by its positive definite square root, then these parallelograms most accurately depict the deformation of a small $(\Delta u, \Delta v)$ rectangle in the parameter plane under the parameterization $\mathbf{x}$ as, e.g., in (6). This qualitatively recovers the discussion about dropped patches, as illustrated in figure 3.

Figure 4 provides a few more examples for visualizing the Riemannian metric for familiar surfaces. Try to squint your eyes and recover the original surface from mentally *patching* together the parallelograms.

This way of visualizing Riemannian metrics is not a totally new idea, but indeed very closely related to the classic *Tissot indicatrix*: This tool has been used extensively in the mid 19th century in cartography and geography, to communicate geometric properties of various projections, such as the Mercator map. For an in-depth discussion of the history and the mathematics of Tissot's indicatrix see, e.g., [20]. It clearly demonstrates the preservation,

or lack thereof, of angles or areas, and showing where the biggest distortions happen, e.g. near the polar regions. Whereas figure 4 employed parallelograms – which indicate the choice of coordinates and bases of the tangent spaces, the more geometric point of view considers distortions of circles (rather than of squares) into ellipses (rather than parallelograms). The next section will adopt this classical choice – at the cost of making it harder *to see* the surface by *squinting*, but more useful for see changes with time as the metric changes according to the Ricci flow.

6 2d Ricci-flow and visualization via Tissot's indicatrix

Whereas the Gauss map $\mathbf{N}\colon S \mapsto S^2 \subseteq \mathbb{R}^3$ defined in section 4 depends on the extrinsic notion of normal vector fields, Gauss showed in his celebrated *Theorema Egregium* in 1827 that the Gauss curvature $K = \det d\mathbf{N}$, the determinant of its differential is *intrinsic*: it only depends on the Riemannian metric, not on the imbedding of the surface into any ambient space. In particular, planes, cones, and cylinders have the same zero Gauss curvature as the latter two may be obtained by rolling up a (part) of the plane.

In higher dimensions, a general notion of curvature for Riemannian manifolds is given by the Riemann curvature tensor Riem, but for many purposes adequate information is provided by the Ricci curvature *tensor* Ricc – which is simply a 2×2 matrix in our context. Starting in the 1980s, foremost Hamilton [13] introduced and analyzed the *Ricci flow*, which is defined as a solution of the partial differential equation

$$\frac{\partial}{\partial t}\, g = -2 \text{ Ricc} \tag{10}$$

In our context g and Ricc are time-varying 2×2 matrices, or rather matrix-valued functions of the parameters/coordinates (e.g., (u, v) or (θ, ϕ)) defining the surfaces/manifolds). This flow was instrumental to Perelman's celebrated proof [21] of the Poincaré Conjecture. It has spawned a huge field of scintillating academic research of analysis of geometric flows.

Since these partial differential equations generally live on higher dimensional abstract manifolds, it is notoriously difficult for nonexperts to visualize such flows. Indeed, technically the flow takes place on the space of Riemannian manifolds, practically on a space of Riemannian metrics, rather than moving points of surfaces in some ambient space. One naturally asks: *"(When) is there hope to* see *this flow as families of surfaces in 3-space evolving with time?"*

Whitney's strong imbedding theorem from 1944 asserts that every smooth manifold M of dimension $n \geq 2$ can be imbedded into $\mathbb{R}^{2n}$ (and can be immersed into $\mathbb{R}^{2n-1}$). [The usual depiction of a Klein bottle in Euclidean 3-space is an immersion, but, due to its self-intersections, not an imbedding.] In our context the most fundamental results are Nash's imbedding theorems, starting with [19], that guarantee that every Riemannian manifold can be isometrically imbedded into some Euclidean space. [Isometric means that the metric the imbedded surface inherits from its ambient space agrees with the Riemannian metric of the original Riemannian manifold.]

Among the vast literature of isometric imbedding theorems, we briefly comment on some that address the case of two-dimensional Riemannian manifolds. Highly technical early work [22, 23] presented theorems of possible imbeddings and counterexamples depending on the degrees of smoothness. The case when the Gaussian curvature changes sign is addressed in

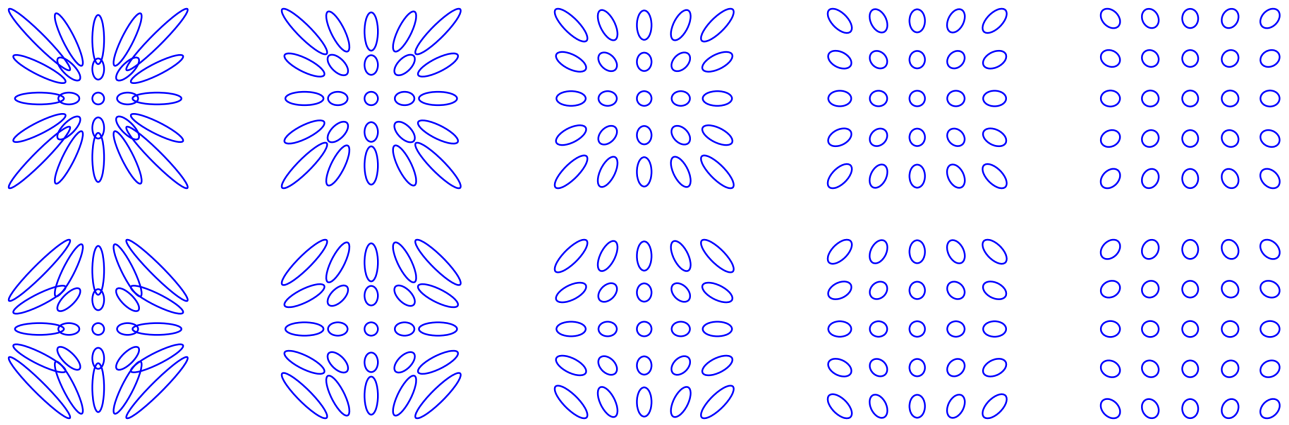

Figure 5: Visualizing of 2d-Ricci flows for initial surfaces $z = x^2 \pm y^2$

[17]. For detailed introductions to the Ricci flow in two dimension see [7] and [15] Some efforts to visualize the two-dimensional Ricci flow are presented in [10]. But we would like to warn the reader about highly counterintuitive results, for example in 2013 it was shown in [5] that the flat torus $T^2 = \mathbb{R}^2/\mathbb{Z}^2$ or $[0,1]^2$ with edges appropriately identified with the flat metric g being the identity can be isometrically imbedded in Euclidean 3-space by a C^1 map.

But in spite of all these positive imbedding theorems one should not expect that in general, even if the *initial value* is an analytic surface in R^3, that the Riemannian manifolds evolving under the Ricci flow have any nice isometric imbedding in R^3 at any time $t > 0$.

Thus instead of focusing on trying to animate the Ricci flow on imbedded surfaces (as in the next section) we have been experimenting with trying to directly visualize the Ricci flow on the space of Riemannian metrics, presented by fields like the Tissot indicatrix. Two typical examples, presented in figure 5, clearly demonstrate the flattening of some bounded parts of a circular and a hyperbolic paraboloid as initial conditions (initial surfaces). We continue to experiment with this new MAPLE worksheet (and will rewrite it in SageMath, too). This again is a small program that is ideally suited for in-class demonstrations, inviting suggestions from students for different initial conditions, and for them to use it for budding research projects. The sample images in figure 5 are proof of concept, but there are many open questions about well-posedness of geometric flows on noncompact surfaces such as these graphs of polynomial functions (there is hope, as they become flat near infinity). The next experiments may involve the standard torus as a surface of revolution, a *double torus* (e.g., a fattened up lemniscate) etc.

7 Ricci flow on surfaces of revolution

While in general it may be hard to predict when the Ricci flow will deform surfaces imbedded in $\mathbb{R}^3$ into surfaces that for every $t \geq 0$ again maybe imbedded in R^3, in 2003 Engman [12] gave a simple necessary and sufficient condition for surfaces of revolution that are homeomorphic to a sphere to have isometric C^1 imbeddings into $\mathbb{R}^3$: The integral of the Gauss curvature over every geodesic disc centered at either pole must be nonnegative. Complementing this, the recent thesis [25] provides a readable survey on intrinsic geometric flows on manifolds of

revolution.

In 2005 Rubinstein and Sinclair [24] demonstrated that 2-dimensional surfaces of revolution homeomorphic to spheres that are initially isometrically imbedded in $\mathbf{R^3}$ remain isometrically imbedded in $\mathbb{R}^3$ for as long as a smooth Ricci flow solution exists. In the same article they presented a numerical simulation of the Ricci flow, with very careful analysis of singularities, which gave rise to captivating series of images of such surfaces under the Ricci flow, that now are ubiquitous on the WWW, even popular on T-shirts.

This section closely follows the numeric implementation of the Ricci flow in this article [24], with new code in SageMath/Python that we have made freely available at GitHub [4]. To give the reader a better idea what this entails, we review some of the construction and terminology used in [24], as well as similar notation.

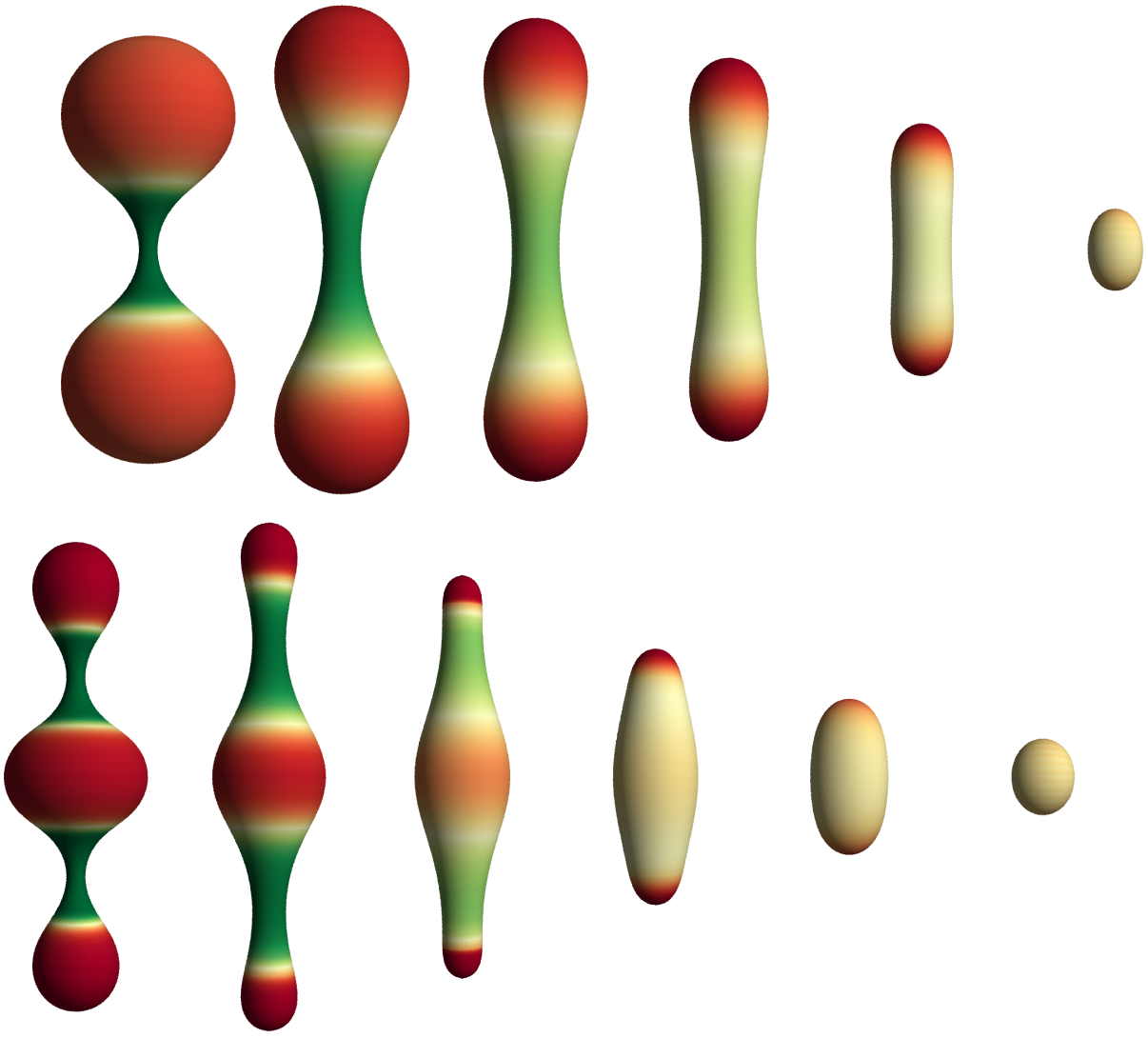

Figure 6: Ricci flow on surfaces of revolution, colored by Gauss curvature.

In the 2-dimensional case the Ricci curvature $\mathrm{Ricc} = K\,g$ is just a scalar multiple of the metric g where K is the Gauss curvature (which n turn depends only, but in an intricate way,

on g and its partial derivatives). Closely following [24] the code `ricci_flow.sage` simulates the Ricci flow on surfaces of revolution, obtained by revolving a parameterized curve $\rho \mapsto (x(\rho), y(\rho))$ in Cartesian coordinates about the first coordinate axes. Think of ρ initially, at time $t = 0$ parameterizing the curve by arclength, but as the curve changes, ρ loses that interpretation.

Whereas the multi-variable calculus exercise asks to calculate the metric for a given parameterized surface, recall that the Ricci flow is takes place at the level of the metric g, and our task is to recover the surface (of revolution) from the metric. Thus we start with an initial metric

$$g_0 = \begin{pmatrix} h_0(\rho) & 0 \\ 0 & m_0(\rho) \end{pmatrix} \tag{11}$$

where for user specified parameters $c_i \geq 0$

$$h_0 \equiv 1, \quad \text{and} \quad m_0(\rho) = \left(\frac{\sin(\rho) + c_3 \sin(3\rho) + c_5 \sin(5\rho)}{1 + 3c_3 + 5c_5} \right)^2 . \tag{12}$$

For any metric g of this diagonal form, i.e., for any $h, m \colon [0, \pi] \mapsto \mathbb{R}_{\geq 0}$ the corresponding curve of revolution as a parameterized curve in Cartesian coordinates is obtained as

$$x(\rho) = \int_0^\rho \sqrt{h(s) - \left(\frac{\partial \sqrt{m(s)}}{\partial s} \right)^2} \, \mathrm{d}s \,, \quad \text{and} \quad y(\rho) = \sqrt{m(\rho)}, \tag{13}$$

At any time $t \geq 0$, given a metric $g = g(t, \rho)$ for $\rho \notin \{0, \pi\}$ the Ricci curvature at that time t, as a function of ρ, may be expressed as

$$\mathrm{Ricc} = \left(-\frac{(\sqrt{m})''}{h\sqrt{m}} + \frac{m'h'}{4mh^2} \right) \begin{pmatrix} m & 0 \\ 0 & h \end{pmatrix} . \tag{14}$$

Because $m(0) = m(\pi) = 0$ and m appears in the denominator of K, these formulae are not used near the singularities, i.e., for $\rho \in [0, \varepsilon)$ and $\rho \in (\pi - \varepsilon, \pi]$, but instead a cubic extrapolation is carried out to close the surface at the poles. To simulate Ricci flow, `ricci_flow.sage` implements a 4th-order Runge-Kutta (RK4) algorithm for the differential equation for Ricci flow (10).

Periodically, reparameterizations are performed in order to prevent numerical instabilities. due to the data points getting too close together as the Ricci flow stretches the surface. In the final frame of each animation in figure 6, the numerical instability near the poles starts to become apparent; ripples can be seen in the color coding by Gauss curvature.

8 `ricci_flow.sage`, SageMath, and classroom technology

The graphics in figure 6 were produced by `ricci_flow.sage`. Mathematically, these evolutions of surfaces closely reproduces the breathtaking results of [24] which are widely familiar, from Wikipedia to T-shirts. The surfaces in these graphics are colored by Gauss curvature: red shades represent positive, and green shades represent negative Gauss curvature.

The `ricci_flow.sage` code, and associated code, is available on GitHub [4]. The code contains numerous variables which control the initial surface shape, the Ricci flow simulation parameters, which plot animations get generated, plot parameters, and camera viewpoint (if saving surface animation frames to individual images). The code is documented, and most

variables are documented by comments. The folder to which images are saved is determined by the `folder_name` variable in the code. The code can be downloaded either by downloading a zip file from its GitHub repository page, or from the command line using `git clone` (if Git is installed). To run the code, SageMath first needs to be installed. The SageMath installation directory can be found at `https://doc.sagemath.org/html/en/installation/index.html`. Once SageMath is installed, `ricci_flow.sage` can be run by opening a terminal and navigating to the `ricci_flow` folder within the cloned/downloaded repository, and running `sage ricci_flow.sage`.

Throughout, `ricci_flow.sage` makes frequent use of built-in SageMath and Python features, including cubic interpolation, numerical integration and differentiation, matrix/vector operations, trigonometric functions, list comprehension, and others. The wide range of available mathematical functions makes the source code for implementing Ricci flow in SageMath far more compact than a similar implementation in a language such as C. Additionally, the free and open-source nature of SageMath along with its Python foundation makes SageMath code far more accessible to students than code written in proprietary languages such as MATHEMATICA and MAPLE would be.

We conclude with some remarks about the choices of technology in mathematics classrooms at the undergraduate (and advanced high school level).

For well over 30 years the 2nd author has relied on and still continues to primarily utilize the commercial symbolic computer algebra systems MAPLE and Mathematics for research and in class for demonstrations and student assignments, from calculus classes to postdoctoral settings. He maintains a very large collection [16] of MAPLE worksheets that are freely available on the WWW, and are regularly used for in-class demonstrations and experimentation, and by students on their own. But the ubiquitous availability of simple graphing applets like DESMOS, as well as freeware such as the free online off-shoot `alpha` of MATHEMATICA, much reduce the need and interest by students to learn the details of the dominant computer algebra systems, and even of MATLAB. Instead, substantial experience in coding in especially the language Python, which is just as old as MAPLE and MATHEMATICA, is rapidly becoming a most valuable marketable skill expected on resumes of our graduates.

The recent substantial expansion and improvement of the Python library `sympy` for symbolic computer algebra led the 2nd author, while still presenting in-class demonstrations in MAPLE, to expect their students to instead try out and complete assignments using `sympy`, Python, and SageMath, starting with vector calculus and differential geometry with their very large algebraic expressions involving many partial derivatives and symbolic inverses of matrices that should always be carried out by machines.

Moreover, the advent of sharing platforms like github introduces students to the necessary insight that no-one can recreate code for all intermediate steps oneself. Students need to learn to make smart decisions on what to code oneself, and when to rely on available libraries, critically evaluating their trustworthiness, and eventually publicly sharing their own work.

9 Acknowledgments.

The authors gratefully thank the two anonymous referees for their careful reading of the manuscript and provident many valuable suggestions for its improvement.

References

[1] Ben Andrews, Bennett Chow, Christine Guenther, and Mat Langford, *Extrinsic geometric flows*, Graduate Studies in Mathematics, vol. 206, American Mathematical Society, Providence, RI, [2020] ©2020.

[2] Sigurd Angenent, *On the formation of singularities in the curve shortening flow*, J. Differential Geom. **33** (1991), no. 3, 601–633.

[3] Catherine Bandle, *Dido's problem and its impact on modern mathematics*, Notices Amer. Math. Soc. **64** (2017), no. 9, 980–984.

[4] Sage Binder, *ricci_flow.sage*, `https://github.com/SageBinder/SageMath-Curvature-Flows`, July 2022, (Accessed on 09/15/2023).

[5] Vincent Borrelli, Saïd Jabrane, Francis Lazarus, and Boris Thibert, *Isometric embeddings of the square flat torus in ambient space*, Ensaios Matemáticos [Mathematical Surveys], vol. 24, Sociedade Brasileira de Matemática, Rio de Janeiro, 2013.

[6] Theodora Bourni, Mat Langford, and Giuseppe Tinaglia, *Collapsing ancient solutions of mean curvature flow*, J. Differential Geom. **119** (2021), no. 2, 187–219.

[7] Paul Bracken, *An introduction to ricci flow for two-dimensional manifolds*, (Albert Baswell, ed.), Advances in Mathematics Research, vol. 22, Nova Science Publishers, 2017, pp. 155–192.

[8] Anthony Carapetis, *curve-shortening-demo,* *https://a.carapetis.com/csf/*, `https://github.com/acarapetis/curve-shortening-demo`, May 2019, (Accessed on 07/30/2023).

[9] Tobias Holck Colding, William P. Minicozzi, II, and Erik Kjæ r Pedersen, *Mean curvature flow*, Bull. Amer. Math. Soc. (N.S.) **52** (2015), no. 2, 297–333.

[10] Junfei Dai, Wei Luo, Min Zhang, Xianfeng Gu, and Shing-Tung Yau, *Visualization of 2-dimensional Ricci flow*, Pure Appl. Math. Q. **9** (2013), no. 3, 417–435.

[11] Manfredo P. do Carmo, *Differential geometry of curves and surfaces*, Prentice-Hall, Inc., Englewood Cliffs, N.J., 1976, Translated from the Portuguese.

[12] Martin Engman, *A note on isometric embeddings of surfaces of revolution*, Amer. Math. Monthly **111** (2004), no. 3, 251–255.

[13] Richard S. Hamilton, *Three-manifolds with positive Ricci curvature*, J. Differential Geometry **17** (1982), no. 2, 255–306.

[14] Cyril Isenberg, *The science of soap films and soap bubbles*, Tieto Ltd., Clevedon, 1978, With a foreword by George Porter.

[15] James Isenberg, Rafe Mazzeo, and Natasa Sesum, *Ricci flow in two dimensions*, Surveys in geometric analysis and relativity, Adv. Lect. Math. (ALM), vol. 20, Int. Press, Somerville, MA, 2011, pp. 259–280.

[16] Matthias Kawski, *Maple worksheet library*, `hhttps://math.la.asu.edu/~kawski/MAPLE/MAPLE.html`, 1995, (Accessed on 09/15/2023).

[17] Chang Shou Lin, *The local isometric embedding in* $\mathbf{R}^3$ *of two-dimensional Riemannian manifolds with Gaussian curvature changing sign cleanly*, Comm. Pure Appl. Math. **39** (1986), no. 6, 867–887.

[18] James McCoy, Glen Wheeler, and Yuhan Wu, *Evolution of closed curves by length-constrained curve diffusion*, Proc. Amer. Math. Soc. **147** (2019), no. 8, 3493–3506.

[19] John Nash, *The imbedding problem for Riemannian manifolds*, Ann. of Math. (2) **63** (1956), 20–63.

[20] Athanase Papadopoulos, *A note on nicolas-auguste tissot: At the origin of quasiconformal mappings*, Handbook of Teichmüller theory. Vol. VII (Athanase Papadopoulos, ed.), IRMA Lectures in Mathematics and Theoretical Physics, vol. 30, European Mathematical Society (EMS), Zürich, 2020, pp. 289–299.

[21] Grigori Perelman, *Ricci flow with surgery on three-manifolds*, arXiv:math.DG/0303109, 2003.

[22] Aleksei Vasilevich Pogorelov, *An example of a two-dimensional Riemannian metric that does not admit a local realization in* E_3, Dokl. Akad. Nauk SSSR (1971), 42–43.

[23] È. G. Poznjak, *Isometric imbedding of two-dimensional Riemannian metrics in Euclidean spaces*, Uspehi Mat. Nauk (1973), no. no. 4(172),, 47–76.

[24] J. Hyam Rubinstein and Robert Sinclair, *Visualizing Ricci flow of manifolds of revolution*, Experiment. Math. **14** (2005), no. 3, 285–298.

[25] Jefferson C. Taft, *Intrinsic geometric flows on manifolds of revolution*, ProQuest LLC, Ann Arbor, MI, 2010, Thesis (Ph.D.)–The University of Arizona.